

# Knowledge Based Brain Tumor Segmentation Graphical User Interface

Kotikalapudi Raviteja, Arun K Gupta, Maya D Bhat, Chandrajit Prasad

**Abstract**—This paper describes a knowledge based brain tumor segmentation system (KBBTS) using histogram interpretations for predicting brain tumor area from trans-axial Magnetic Resonance Imaging (MRI). A graphical user interface (GUI) was developed for the segmentation of brain tumor images. This system showed significant improvements over traditional threshold-based tumor segmentation methods. Although KBBTS is not designed to work in real time, it serves as potential research advancement for real time brain tumor segmentation using computer-aided systems with high performance.

**Index Terms**—Glioma, graphical user interface (GUI), histogram, knowledge based brain tumor segmentation (KBBTS), trans-axial magnetic resonance imaging (MRI)

## I. INTRODUCTION

Glial neoplasms constitute more than 70% of primary malignant brain tumors, and result in more years of life lost compared to any other tumors [17]. Astrocytic tumors are the most frequent variety, making up more than three-quarters of all gliomas [15]. They are classified into four grades (I, II, III and IV), and the treatment and prognosis depends upon the tumor grade [16].

These are heterogeneous group of tumor vary from well circumscribed to highly infiltrative. Malignant tumor with its infiltrative nature makes it difficult to define on imaging however affect the image-pixel values particularly at the boundary and boundary-surrounding locations of the tumor. As a result, a quality knowledge based system becomes highly potential in supporting manual or automated tumor detection.

A classical approach where radiologists makes a subjective assessment and marks the tumor manually on MR images, is called manual tumor marking. Besides being a time-taking task for doctors, it does have an element of subjectivity hence it becomes important to challenge ourselves in advanced science and technology to develop a computer-based automated tool for continuing the same process with increased efficiency. Automated model which would use logic algorithms and knowledge base of radiologist and image processors could certainly prove to be a potential system for segmenting brain tumors.

**Manuscript received December, 2013.**

**Kotikalapudi Raviteja**, Junior Research Fellow, Neuroimaging and Interventional Radiology, National Institute of Mental Health and Neurosciences, Bangalore, India.

**Dr. Arun K Gupta**, Professor and Head, Neuroimaging and Interventional Radiology, National Institute of Mental Health and Neurosciences, Bangalore, India.

**Dr. Maya D Bhat**, Assistant Professor, Neuroimaging and Interventional Radiology, National Institute of Mental Health and Neurosciences, Bangalore, India.

**Dr. Chandrajit Prasad** (corresponding author), Assistant Professor, Neuroimaging and Interventional Radiology, National Institute of Mental Health and Neurosciences, Bangalore, India.

With the aid of medical imaging and computer programming, automated tumor segmentation could immensely contribute to better diagnosis, accurate treatment and surgery planning in lesser time leading to increased life span of tumor survivors.

The primary aim of this paper was to design and develop a Graphical User Interface (GUI) for knowledge based automated tumor segmentation which would separate tumor from non-tumor areas through automated histogram curve interpretations.

The rest of the paper is divided into four sections. Section II reviews previous works in relevance to the aims of our research. Section III describes several algorithms forming the GUI and its experimentation on glioma data sets. Section IV presents the results for performance of our GUI in comparison with the ground truth, followed by experimental results, conclusion and future works.

## II. REVIEW OF PREVIOUS WORKS

To the best of our knowledge, majority of efficient methods and comparative studies pertaining to brain segmentation were based on neural networks, fuzzy logic, region growing algorithms, segmentation by simple thresholding and knowledge based algorithms [3], [2]. The method proposed by MK Kowar and S Yadav, segments the tumor using histogram threshold technique [6]. In this method, presumption of thresholding completely depends on human visual interpretation which could significantly decrease the accuracy by gaining non-tumor pixels or losing tumor pixels in the segmented image. User interface tools have also been proposed previously to segment low-grade gliomas and extra-axial tumors like meningiomas [5]. It assures high speed segmentation but the system might suffer low accuracy levels in case of high grade tumors. MC Clark et al., developed a model for tumor segmentation using knowledge based techniques [4]. The method showed significant results when compared with the ground-truth but was limited to three subjects. As a result, it is difficult to say if the method would be efficient over larger number of data sets. J Zhou et al., proposed a one-class support vector machine (SVM) for effective brain tumor segmentation [14]. But when J Zhang et al., compared it with two-class SVM, the later produced less false positives because of the separation information derived from tumor and non-tumor data [13]. Hence, the overall specificity of the model is reduced. WE Reddick et al., used artificial neural networks for automated segmentation and classification of magnetic resonance images [8]. The method was a hybrid neural network combining Kohonen self-organizing neural networks and multi-layer back-propagation neural networks. Gradient vector flow (GVF), Magneto-static active contour (MAC) and Fluid vector flow (FVF) has been implemented for segmentation of homogeneous tumors [10-12]. But these models fail to significantly differentiate tumors from similar background intensities. Such problems have been addressed

by J Sachdeva et al., by developing a content-based active contour model (CBAC) where intensity and as well as texture inputs are taken from the active contour [9].

A variety of algorithms and their combinations to form hybrid algorithms have been used in previous literature. Having said that, these works have widely been experimental, yet to be put in diagnostic use. Hence it gives us further scope to research brain tumor segmentation using automated models.

### III. PROPOSED WORK

The proposed work is a series of steps involved in segmenting brain tumor using KBBTS. Data acquisition, pre-processing, tumor segmentation, morphological operations and location-window filtering form the basic logical components of the GUI. Fig 1 shows the block diagram of the proposed work.

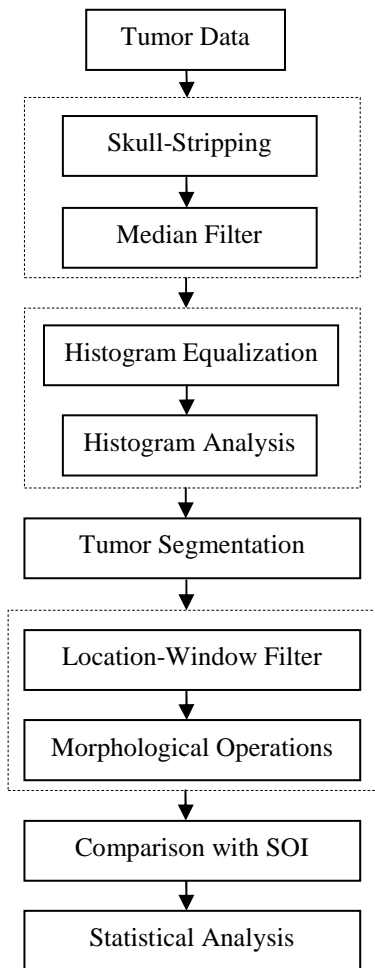


**Fig 1: Block diagram of the proposed work divided into five steps viz., acquisition, pre-processing, information analysis, post-processing and statistical analysis.**

#### A. Data

Data was acquired in the form of DICOM images. These images were converted to NIFTI format using dcm2niiGUI software (available from [www.mccauslandcenter.sc.edu](http://www.mccauslandcenter.sc.edu)). The tumor slices of interest in NIFTI format were then saved as .TIFF format images using MRI Cro (available from [www.mristudio.org](http://www.mristudio.org)).

#### B. Software application

MATLAB R2010a (developed by MathWorks) was used for the design and development of the GUI. Image processing, histogram analysis and statistical analysis were also carried out by the same software.

#### C. Image pre-processing

Implementing skull-stripping and median filtering were the two steps involving pre-processing of tumor images.

##### Skull-stripping

Non-cerebral bony tissues such as the skull were removed. The process is often referred to as skull stripping. It was successfully executed using the software, MRI Cro. A certified radiologist carefully selected the slices-of-interest (SOI) for further study. The SOIs were saved in TIFF format which then consisted of pixel intensity values in x- and y-directions, later to be used for 2-D tumor segmentation.

##### Median Filter

It is important to remove unwanted information, in this case; the noise filled pixels. 2D-Median filter was used for the reduction of salt and pepper noise from the image. It reduces the noise and preserves edges at the same time. The equation used for performing median filtering is given below:

$$f(x, y) = \text{median} \{g(s, t) \mid (s, t) \in S_{xy}\} \quad (1)$$

#### D. Histogram analysis

Histogram equalization, histogram smoothing and identifying the lower and upper threshold formed the histogram analysis.

##### Histogram Equalization

Image enhancement was performed by enhancing pixel intensities using Contrast-Limited Adaptive Histogram Equalization (CLAHE). Rather than the entire image, CLAHE operates on small pixel groups in the image which are known as tiles. The following command was used for image enhancement:

$$\text{EnhancedImage} = \text{adaphisteq}(\text{Image}); \quad (2)$$

##### Local Regression Smoothing (LOESS)

Histogram smoothing was done by local regression smoothing algorithm. Regression weights for each data point were calculated using the following equation:

$$w_i = \left[ 1 - \left| \frac{x - x_i}{d(x)} \right|^3 \right]^3 \quad (3)$$

where  $x$  is the assigned predictor value, which is associated with response value (to be smoothed). The nearest neighbors of  $x$  were  $x_i$  ( $i = 1, 2, 3, \dots, n$ ). The distance between  $x$  and the most distance predictor value is  $d(x)$ . A weighted linear least squares regression was performed. In case of loess, a second degree polynomial function was used by the regression. This allowed us to accurately select lower threshold ( $T_{min}$ ) and upper threshold ( $T_{max}$ ).

##### Identifying $T_{min}$ and $T_{max}$

The histogram of the image was represented by the function, histogram ( $i$ ), where  $i$  is an integer between 0 and 255. The finding of global thresholds is described in the following steps:

- 1) The first step was to generate a histogram matrix; histogram ( $m, 1$ ) where  $m$  was the number of pixels. A zero matrix; peaks ( $m, 1$ ) was also created.
- 2) Local histogram peaks were calculated through the following condition:

**if histogram (i) > histogram (i+1) &&  
 histogram (i) > histogram (i-1);  
 peaks (i) = histogram (i);  
 else peaks (i) = 0;**

This step was repeated for a second time in order to further filtering the peaks and retaining clinically significant peaks.

3) We compared the second maximum number of pixels; histogram<sub>2max</sub> with the existing peaks to eliminate peaks which were very small compared to histogram<sub>2max</sub>. The following condition was used to eliminate non-significant peaks:

**if [peaks (i) / (histogram<sub>2max</sub>)]\*100 < 10;  
 peaks (i) = histogram (i);  
 else peaks (i) = 0;**

We observed that the maximum number of pixels was having an intensity value of zero, a majority of which was background. Hence, second maximum value was considered for the condition.

4) Now, minimum and maximum values for each served as the threshold value to segment the image into white matter, gray matter, edema, tumor and necrosis. The two thresholds for tumor segmentation were taken as **T<sub>min</sub>** and **T<sub>max</sub>**.

#### E. Tumor segmentation

One of the key concepts used in the implementation of tumor segmentation algorithm was the range of pixel intensities in TIFF format images. The intensity range is specified as:

**PixIntensity<sub>black</sub> = 0 to PixIntensity<sub>white</sub> = 255**

Hence, every pixel identified in the image would fall in a range which is the subset of the intensity range. For each range subset, there was a **T<sub>min</sub>** and **T<sub>max</sub>** which represented an entire region of the brain. After determining the values for **T<sub>min</sub>** and **T<sub>max</sub>**, following steps segmented the tumor:

- 1) Read **T<sub>min</sub>** and **T<sub>max</sub>**
- 2) Calculated image size = m × n; EnhancedImage [m, n]
- 3) Create SegmentedImage; a zero matrix for size = m × n and the following condition was applied:  
**for i = 1:m**  
**for j = 1:n**  
**if EnhancedImage [i, j] > T<sub>min</sub>**  
**&& EnhancedImage [i, j] < T<sub>max</sub>**  
**SegmentedImage [i, j] = 1;**  
**else SegmentedImage [i, j] = 0;**  
**end**  
**end**  
**end**

This algorithm considered a single matrix element of tumor slice and designated a pixel value of either 1 (white) or 0 (black) on satisfying the above mentioned condition. The algorithm is an iterative process which runs till it reaches the last element of the matrix.

#### F. Location-window filtering

A location window filter algorithm was developed in order to remove non-tumor regions and speckles created after segmentation. The algorithm makes use of location co-ordinates and window size as the inputs.

The position of the pixel was considered as the location information. Window was split into four quadrants namely (X)(Y), (-X)(-Y), (X)(-Y) and (-X)(Y). Hence, location values for the windows were considered as  $(x,y) \in Q_{(x,y)}$ ,

$(-x,-y) \in Q_{(-x,-y)}$ ,  $(x,-y) \in Q_{(x,-y)}$  and  $(-x,y) \in Q_{(-x,y)}$  respectively. The size of each window varies for a given value of x and y in all the four directions.

#### G. Morphological operations

We implemented erosion and dilation as two features of morphological operations on segmented images. Erosion refers to decrease in size and dilation refers to increase in size. As a result, erosion removes pixels from the boundary of the image and dilation adds pixels to the boundary of the image.

If A and B are sets in  $Z^2$ , the equation for dilation of A by B is given by:

$$A \oplus B = \{z | [(B)_z \cap A] \subseteq A\} \quad (4)$$

The equation denoting the erosion of A by B is given by:

$$A \ominus B = \{z | (B)_z \subseteq A\} \quad (5)$$

where A represents the image matrix on which morphological operations were performed and B represents the structuring element in morphological operations. z denotes the displacements.

#### H. GUI for hand-labeling of tumor

A GUI was developed for the manual labeling of SOIs. All the SOIs were hand-labeled by 2 certified radiologists. The marking of tumor was done manually. Labeled images were then used for further comparison with machine generated images and statistical analysis was performed. A brief code for the GUI has been supplied below:

```
global roiImage;  
image = handles.image;  
roiImage = roipoly (image);  
axes (handles.axes2);  
imshow (roiImage);
```

#### I. Statistical analysis

Sensitivity and Specificity are the two prime performance parameters used in medical statistics. Sensitivity denotes the value which is the number of patients who were correctly identified with a disease [8], [1]. Specificity denotes the value which is the number of patients who were correctly identified as not having a disease [8], [1]. The equations for calculating sensitivity and specificity are:

$$\text{Sensitivity} = TP / (TP + FN)$$

$$\text{Specificity} = TN / (TN + FP)$$

where True Positive (TP) indicates that patient suffered diseases and result was positive; True Negative (TN) indicates that patient did not suffer disease and result was negative; False Positive (FP) indicates that patient did not suffer disease and result was positive; False Negative (FN) indicates that patient suffered disease and result was negative.

Accuracy of a system can be referred to as the system's ability to produce the actual results. A system with higher accuracy is reliable than a system with lower accuracy. In this project, accuracy is defined by the following equation:

$$\text{Accuracy} = TP + TN / (TP + TN + FP + FN)$$

Positive Predictive Value (PPV) is defined as the proportion of patients tested positive that actually have the disease [8], [1]. It is referred to as the precision rate.

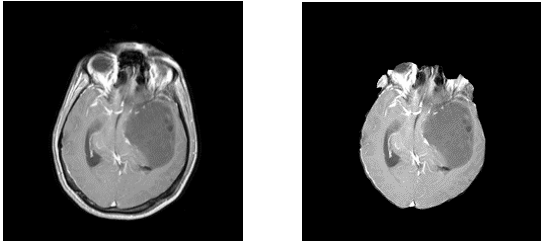
$$\text{PPV} = TP / (TP + FP)$$

Negative Predictive Value (NPV) is defined as the proportion of patients tested negative who actually do not have the disease [7], [1].

$$NPV = TN / (FN + TN)$$

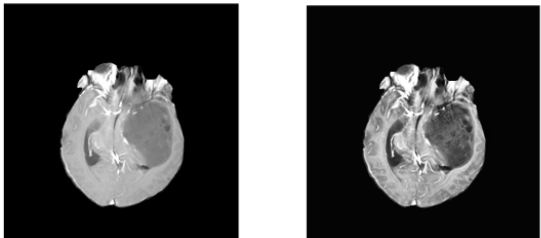
IV. EXPERIMENTAL RESULTS

This section presents all the results generated by the KBBTS.



(a) Before (b) After

Fig 1: The figures show the effect of skull-stripping on T1 post Gd image while using FFE sequence.



(a) Before (b) After

Fig 2: The figures show the effect of image enhancement by adaptive histogram equalization

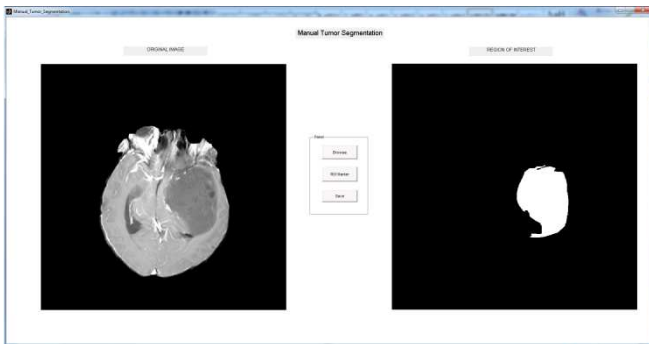


Fig 3: GUI for hand-labeling of tumor

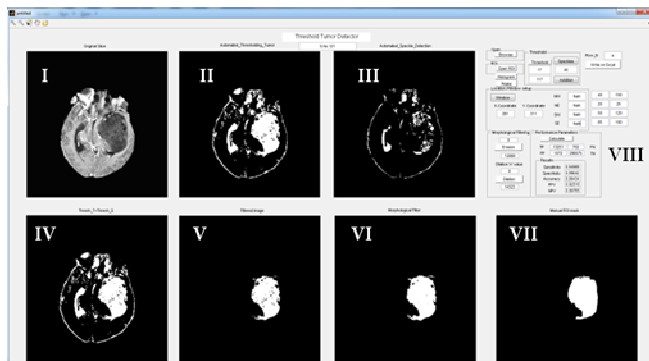


Fig 4: Knowledge Based Brain Tumor System: I displays the slice of interest, II is the viewer for Black-and-White image obtained after histogram analysis, III is the viewer for speckles/black spots left in the tumor. IV displays adding the threshold image and speckles, V displays the effect of location-window filtering, VI shows the image obtained after morphological operations, VII displays the hand-labeled tumor

ROI used for comparison with the GUI output image and VIII is the operating panel for image browser, threshold selection, location-window filtering, morphological operation options, and performance parameters.

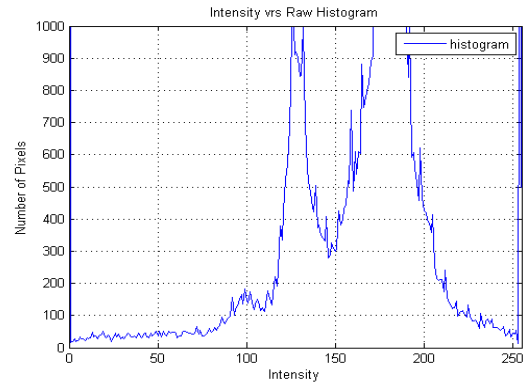


Fig 5: The figure shows the raw histogram of the image. The presence of consistent peaks throughout the histogram makes it difficult to identify tumor, white matter, grey matter and CSF.

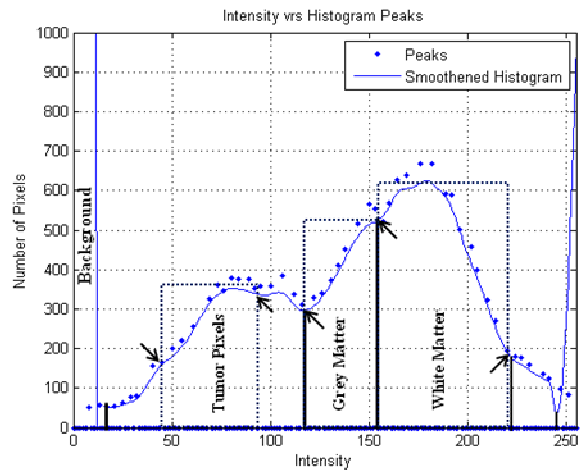


Fig 6: Processed histogram for an efficient identification of tumor thresholds. The figure shows a detailed break-down of the histogram curve with each threshold range pertaining to A certain region of brain.

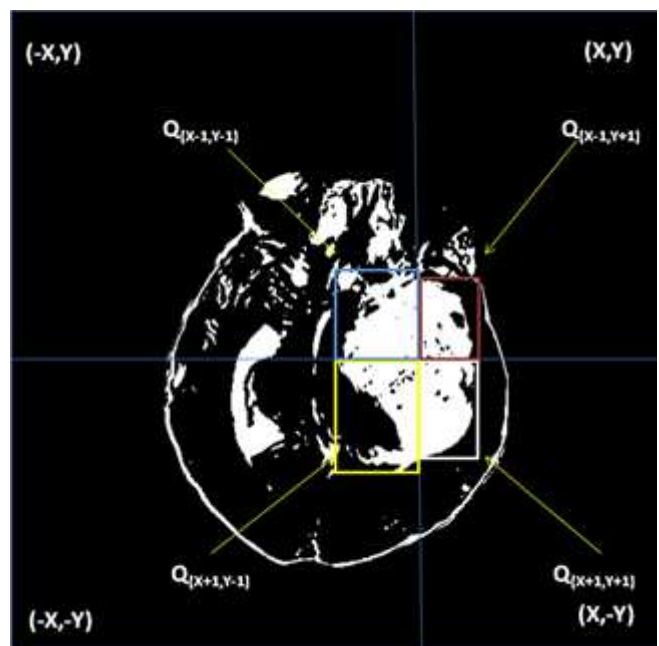
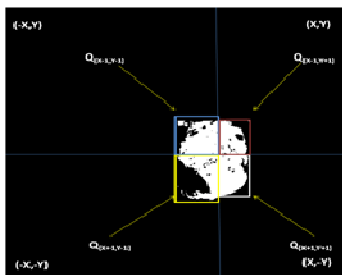
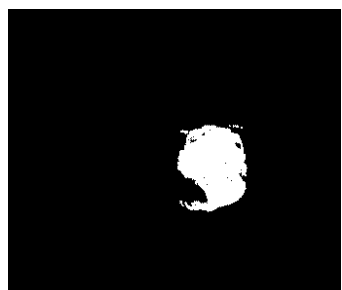


Fig 7: Location-Window filtering: The image represents four windows in four quadrants covering the entire tumor.





**Fig 8: Effect of Location-Window filter:** The implementation of the filter resulted in accepting the tumor pixels and rejecting pixels falling outside the windows.



**Fig 9: Output image after morphological operations:** It could be clearly observed from the image that most of the black speckles were consistently filled inside the tumor through low level morphological dilation. The area of the tumor could now be calculated by counting the number of white pixels (pixValue =1).

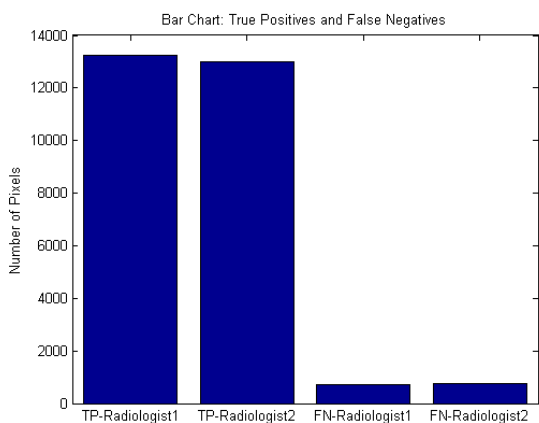


**Fig 10: Average number of True Positives and False Negatives generated by KBBTS.**

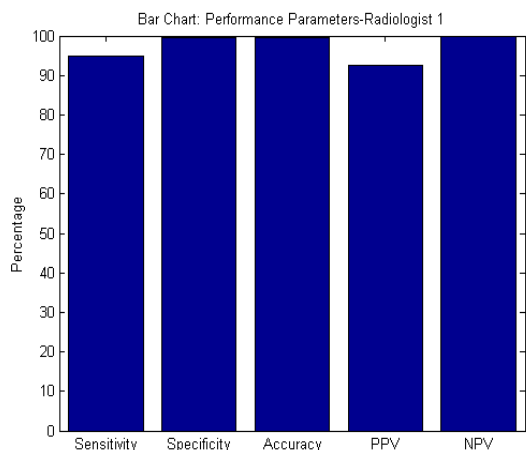


**Fig 11: Performance analysis when compared with tumor labeled by Radiologist 1.**

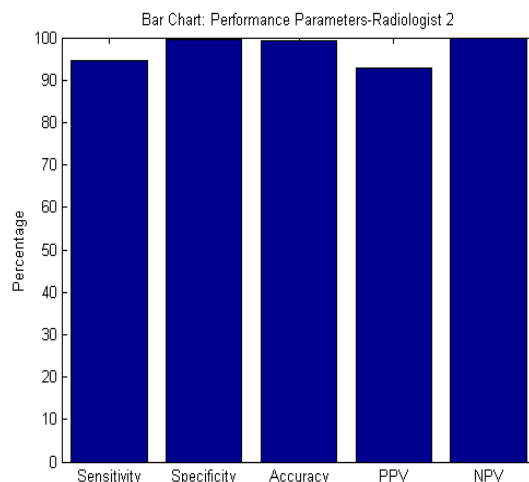


**Fig 12: Performance analysis when compared with tumor labeled by Radiologist 2.**

### V. CONCLUSIONS

In this paper we have presented a Knowledge Based Brain Tumor segmentation system. It was designed, tested and evaluated for efficient brain tumor segmentation. Two radiologists hand-labeled the tumor slices of interest and performance parameters were drawn by comparing these manually labeled slices with the ones generated by KBBTS. The images shown in the results showed that the system was successful in segmenting the tumor from healthy brain pixels. From Table 1, the mean values for sensitivity, specificity, accuracy, PPV and NPV were found to be 94.79%, 99.6%, and 99.39%, 91.64% and 99.76% respectively

**Table 1: KBBTS Performance analysis**

Performance	Radiologist 1	Radiologist 2
True Positives	13251	13002
True Negatives	298575	298538
False Positives	1072	1321
False Negatives	702	739
Sensitivity	94.96	94.62
Specificity	99.64	99.55
Accuracy	99.43	99.34
PPV	92.51	90.77
NPV	99.77	99.75

### VI. FUTURE WORK

Prior knowledge for recognizing minima and maxima of curves was considered as the primary base for detecting lower and upper thresholds between which most of the tumor pixels were present. In this case, a completely automated GUI for recognizing tumor pixels from histogram should be developed. The system could successfully segment 2-D tumors from all the slices. This particular methodology should be implemented for 3-D tumor segmentation. We have tested the system for brain tumor images. KBBTS should also be tested for tumors occurring outside the brain.

### REFERENCES

[1] Anthony K Akobeng. Understanding diagnostic tests 1: sensitivity, specificity and predictive values. Acta paediatrica, 96(3):338-341, 2007.

- [2] Mohd Ali Balafar, Abdul Rahman Ramli, M Iqbal Saripan, and Syamsiah Mashohor. Review of brain mri image segmentation methods. *Artificial Intelligence Review*, 33(3):261-274, 2010.
- [3] Samir Kumar Bandhyopadhyay and Tuhin Utsab Paul. Segmentation of brain mri image-a review. *International Journal*, 2(3), 2012.
- [4] Matthew C Clark, Lawrence O Hall, Dmitry B Goldgof, Robert Velthuizen, F Reed Murtagh, and Martin S. Silbiger. Automatic tumor segmentation using knowledge-based techniques. *Medical Imaging, IEEE Transactions on*, 17(2):187-201, 1998.
- [5] Michael R. Kaus, Simon K. War\_eld, Arya Nabavi, Peter M. Black, Ferenc A. Jolesz, and Ron Kikinis. Automated segmentation of mr images of brain tumors. *Radiology*, 218(2):586-591, 2001. PMID: 11161183.
- [6] Manoj K Kowar and Sourabh Yadav. Brain tumor detection and segmentation using histogram thresholding. *IJEAT ISSN*, pages 2249-8958, 2012.
- [7] Rajul Parikh, Annie Mathai, Shefali Parikh, G Chandra Sekhar, and Ravi Thomas. Understanding and using sensitivity, specificity and predictive values. *Indian journal of ophthalmology*, 56(1):45, 2008.
- [8] Wilburn E Reddick, John O Glass, Edwin N Cook, T David Elkin, and Russell J Deaton. Automated segmentation and classification of multispectral magnetic resonance images of brain using artificial neural networks. *Medical Imaging, IEEE Transactions on*, 16(6):911-918, 1997.
- [9] Jainy Sachdeva, Vinod Kumar, Indra Gupta, Niranjana Khandelwal, and Chirag Kamal Ahuja. A novel content-based active contour model for brain tumor segmentation. *Magnetic resonance imaging*, 30(5):694-715, 2012.
- [10] Tao Wang, Irene Cheng, and Anup Basu. Fluid vector flow and applications in brain tumor segmentation. *Biomedical Engineering, IEEE Transactions on*, 56(3):781-789, 2009.
- [11] Xianghua Xie and Majid Mirmehdi. Mac: Magnetostatic active contour model. *Pattern Analysis and Machine Intelligence, IEEE Transactions on*, 30(4):632-646, 2008.
- [12] Chenyang Xu and Jerry L Prince. Gradient vector Flow: A new external force for snakes. In *Computer Vision and Pattern Recognition, 1997. Proceedings., 1997 IEEE Computer Society Conference on*, pages 66-71. IEEE, 1997.
- [13] Jianguo Zhang, Kai-Kuang Ma, Meng-Hwa Er, Vincent Chong, et al. Tumor segmentation from magnetic resonance imaging by learning via one-class support vector machine. In *International Workshop on Advanced Image Technology (IWAIT'04)*, pages 207-211, 2004.
- [14] J Zhou, KL Chan, VFH Chong, and SM Krishnan. Extraction of brain tumor from mr images using one-class support vector machine. In *Engineering in Medicine and Biology Society, 2005. IEEE-EMBS 2005. 27th Annual International Conference of the*, pages 6411-6414. IEEE, 2006.
- [15] Burger PC, Vogel FS. The brain: tumors In: Burger PC, Vogel FS, eds. *Surgical pathology of the central nervous system and its coverings*. New York, NY: Wiley, pages 223-266, 1982.
- [16] Pathology and genetics of tumours of the nervous system. In: *World Health Organization Classification of Tumours of the Nervous System, Editorial and Consensus Conference Working Group. Kleihues, P, Cavenee, WK (Eds), IARC Press, Lyon, France 2000.*
- [17] Ohgaki, Hiroko, and Paul Kleihues. Epidemiology and etiology of gliomas. *Acta neuropathologica* 109(1): 93-108, 2005.